Characterization by EXAFS of Co/MFI catalysts prepared by sublimation

ARTICLE *in* THE JOURNAL OF PHYSICAL CHEMISTRY B · JUNE 2002

Impact Factor: 3.3 · DOI: 10.1021/jp020870y

Characterization by EXAFS of Co/MFI Catalysts Prepared by Sublimation

V. Schwartz,[†] R. Prins,[†] X. Wang,[‡,§] and W. M. H. Sachtler*[,§]

Technisch-Chemisches Laboratorium ETH-Zentrum, CH-8092 Zürich, Switzerland, and Catalysis Center, Northwestern University, Evanston, Illinois 60208-3000

Received: April 2, 2002; In Final Form: May 17, 2002

Catalysts have been prepared by subliming $CoCl_2$ or $CoBr_2$ vapor onto the H form of the zeolite MFI, followed by replacing the halide ions by OH groups and subsequent heat treatments. The Co sites have been characterized by EXAFS and XANES spectra at liquid nitrogen temperature. The data are correlated with the H_2-TPR profiles of the same samples and their catalytic performance in reducing NO_x with hydrocarbons. Materials with fairly large Co_3O_4 particles after calcination, displaying a Co−Co distance of 3.5 Å and negligible interaction between Co and T sites (T = Si or Al), have a poor selectivity in NO_x reduction, because such oxide particles catalyze the combustion of the hydrocarbon. In contrast, highly selective catalysts show no Co_3O_4 clusters and distinct interaction between Co and T atoms. Heating in H_2 at 400 °C reduces Co−oxo ions, while cobalt oxide clusters are incompletely reduced and isolated Co^{2+} ions in exchange positions remain unreduced. The water formed in the reduction of oxo species can interact with Co^{2+} ions, increasing their coordination number with oxygen. A preedge XANES peak at 7710 eV indicates an electric-dipole-forbidden, but quadrupole-allowed and vibronically allowed 1s−3d electronic transition.

1. Introduction

Zeolite-supported cobalt catalysts are remarkably active in the reduction of nitrogen oxides. Not only do they achieve high conversion of NO_x to N_2 in the presence of a large excess of oxygen, but they are also capable of catalyzing NO_x reduction with methane as the sole reductant.[1,2] This distinguishes them from zeolite-based catalysts with Cu or Fe as the active ingredient, which require higher alkanes or alkenes as the reducing hydrocarbon. Various techniques have been applied to characterize the cobalt sites in zeolite MFI or ferrierite. It appears that the activity and selectivity of the catalysts critically depends on the metal loading and the technique by which the catalysts were prepared. Basically, two main types can be discerned.

(1) Catalysts prepared by ion exchange from aqueous solution. This method leads to materials with rather low loading; the molar ratio of cobalt to aluminum in the zeolite framework is ≤0.5. Such catalysts have been extensively characterized by the group of B. Wichterlová.[3,4]

(2) Catalysts prepared by sublimation of a volatile cobalt halide onto the H form of the zeolite. They typically have Co/Al molar ratios near unity and are the focus of the EXAFS analysis in the present paper. Catalytic tests and characterization by TPR of materials prepared by *sublimation* of cobalt chloride or bromide vapor onto H-MFI have been described in previous papers.[5,6] The results indicate the presence of at least three types of cobalt sites after treatment with water (to replace most halide ions by hydroxyl ions) and calcination. The nature of these sites was inferred from a comparison of the TPR profiles with those of catalysts prepared by conventional ion exchange from aqueous solution or by impregnation.

This assignment of H_2-TPR peaks to cobalt sites is illustrated in Figure 1. The track marked WIE shows the typical pattern of a catalyst prepared by conventional "wet" ion exchange. Only one reduction peak at about 700 °C is prominent. It has been assigned to isolated Co^{2+} ions. Formation of Co°_n nuclei and protons is the rate-limiting step in catalyst reduction; it requires a high temperature. For the catalyst prepared by sublimation from $CoCl_2$ a TPR peak at 385 °C is prominent; other features are observed at even lower temperatures. The 385 °C peak is also found with samples prepared by impregnation on Na/MFI, for which XRD had shown the presence of Co_3O_4 particles. This suggests that such particles are also present in the material prepared by sublimation from $CoCl_2$. Formation of Co−Co bonds will be much easier when oxide particles are reduced which contain Co ions as next nearest neighbors than by reducing isolated Co^{2+} ions in zeolite cavities. A third species is indicated by TPR peaks at even lower temperature. This has been ascribed to easily reducible configurations containing two or more Co ions in each other's close proximity, such as the dinuclear oxo ions $[Co-O-Co]^{2+}$.

Figure 1 also shows that none of the materials described in refs 5 and 6 show significant reduction in the wide temperature window between the 385 and 700 °C peaks. This suggests that hydrogen treatment at a temperature inside this window should selectively reduce cobalt oxide particles and easily reducible oxo ions, but leave isolated Co^{2+} ions unreduced. It is, therefore, of interest to compare samples that were treated in either H_2 or O_2 at 400 °C.

One objective of the present work is to compare materials made by sublimation of either $CoCl_2$ or $CoBr_2$. The bromide has a higher vapor pressure than the chloride; in Figure 1 the TPR tracks of the catalysts prepared from either halide show clear differences which are not easily interpreted. It is also of interest to compare catalysts that were made in a similar manner but showed different performances, revealing the importance of subtle differences in sublimation conditions. Two Co/MFI catalysts were included in this study that were prepared by sublimation from cobalt chloride, but for which the catalysis

* To whom correspondence should be addressed.
† Technisch-Chemisches Laboratorium ETH-Zentrum.
‡ Present address: Department of Chemical Engineering, University of Pennsylvania, Philadelphia, PA19104-6393.
§ Northwestern University.

10.1021/jp020870y CCC: $22.00
Published on Web 06/27/2002

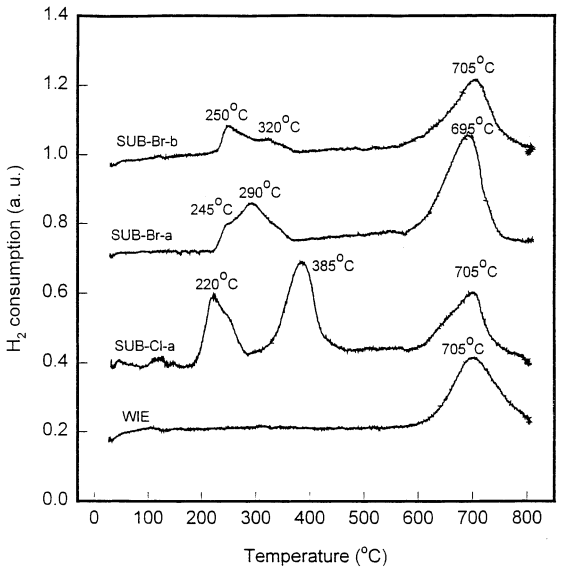

Figure 1. H_2 TPR profile of Co/MFI catalysts. Reprinted with permission from ref 5. Copyright 2000 Elsevier Science. WIE = prepared by "wet" ion exchange, SUB-Cl-a = prepared by sublimation of $CoCl_2$ on H-MFI with Si/Al = 14, SUB-Br-a = prepared by sublimation of $CoBr_2$ on H-MFI with Si/Al = 14, and SUB-Br-b = prepared by sublimation of $CoBr_2$ on H-MFI with Si/Al = 19.

test revealed differences. One catalyst, further called CZO3, displayed a high conversion of NO to N_2, whereas the other, called CZO5, mainly catalyzed combustion of the hydrocarbon. Obviously it is of great interest to know the cause for this difference in catalytic performance.

On summarizing, the present study will focus on three materials, prepared by sublimation of a cobalt halide onto H-MFI:

CZO3 prepared from $CoCl_2$ and showing a good catalytic performance, described in refs 5 and 6,

CZO5 prepared from $CoCl_2$ but showing a much poorer catalytic performance, and

$CZBrO_2$ prepared from $CoBr_2$ and showing a good performance described in ref 5.

2. Experimental Section

Catalyst preparation by sublimation from $CoCl_2$ or $CoBr_2$ has been described previously.[5,6] Sublimation of $CoCl_2$ was, typically, carried out in an Ar flow at 100 mL/min at 700 °C for 72 h; with $CoBr_2$ 50 h at 600 °C was found sufficient. The samples were thoroughly washed with water, followed by drying in air, before they were shipped to Zurich, where they were pressed into self-supported wafers and mounted in an in situ EXAFS cell. The sample thicknesses corresponded to an edge jump equal to 1 for the Co K edge. For each sample, a pretreatment in either flowing O_2 or flowing H_2 was carried out prior to the measurements. The flow rate of the O_2 or H_2 was 50 cm^3/min at amospheric pressure. During this treatment, the temperature was raised uniformly at a rate of 5 °C/min from room temperature to 400 °C, and held at 400 °C for 1 h. After each treatment, the cell was purged with helium at room temperature and cooled to liquid nitrogen temperature for all the measurements.

The EXAFS data at the Co K edge were collected at the Swiss Norwegian Beam Line (SNBL, BM1) at the European Synchrotron Radiation Facility (ESFR), Grenoble, France. The electron energy was 6.0 GeV, and the ring current was between 90 and 200 mA. A Si(111) crystal was used as a channel-cut monochromator, and a gold mirror was employed to reject harmonics. The X-ray absorption was measured by the incoming (I_o) and transmitted (I_t) beams, which were detected by ion chambers. The chambers for measuring I_o and I_t were 17 and 31 cm long, and the I_o ion chamber was filled with pure N_2 whereas the I_t ion chamber was filled with a mixture of Ar/N_2 = 35/65 (vol %). For the measurements, the scans were divided into six regions: 7159−7659 eV (preedge), 7659−7759 eV (edge region), 7759−7870 eV (postedge, k = 3.6−6.5 $Å^{-1}$), 7870−8090 eV (postedge, k = 6.5−10 $Å^{-1}$), 8090−8566 eV (postedge, k = 10−15 $Å^{-1}$), and 8566−8810 eV (postedge, k = 15−17 $Å^{-1}$). The collection time for each data point in each scan region was 1, 1, 2, 3, 5, and 6 s, respectively.

The EXAFS data were analyzed using the XDAP program (version 2.2.3).[7] In short, the data reduction procedure consisted of the following steps: spectra averaging, preedge subtraction, background determination, and normalization. First, three scans were measured and averaged. Then, the preedge background was approximated by a modified Victoreen curve, and the background was subtracted using a cubic spline routine. Finally, the spectra were normalized by the edge jump. The k^3-weighted and k^1-weighted EXAFS functions were Fourier transformed and fitted in R space. The interatomic distance (R), the coordination number (CN), the difference of the Debye−Waller factor from the reference ($\Delta\sigma^2$), and the correction of the threshold energy ($\Delta E°$) were treated as free parameters during the fitting. The quality of the fit was estimated from the values of variance and goodness of the fit (ϵ_v^2). The variance represents the residual between the observed and calculated spectra in the fitted range. For the imaginary and absolute parts, the variances V_{IM} and V_{ABS} were calculated in R space applying the same weight factor used for the fitting. The ϵ_v^2 value takes the number of free parameters into account and is used to determine whether the addition of new parameters makes sense. Therefore, ϵ_v^2 has only a relative meaning permitting comparison of the quality of the fit in the same spectra and with the same k weighting with different parameters. The smaller the ϵ_v^2, the better the fit. To analyze the spectra, phase shifts and the backscattering amplitude from reference compounds were used. The Ni−Ni coordination in NiO was used as a reference for Co−Co, since the phase shift and backscattering amplitude of Ni and Co hardly differ. In the case of Co−O and Co−Si/Al coordination, a theoretical reference was calculated with FEFF7,[8] on the basis of crystallographic data of CoO and Co_2SiO_4.

3. Results

Figure 2 shows the absolute parts of the Fourier-transformed $\chi(k)\cdot k^3$ Co K-edge EXAFS functions of all the catalysts after O_2 treatment (Figure 2a) and after H_2 treatment (Figure 2b) at 400 °C in the range of 3.5 Å < k <12.5 Å. The spectra of Co_2SiO_4, CoO, and Co_3O_4, simulated with FEFF7, are also included. The Fourier transform of the $CZBrO_2$ sample after H_2 treatment is similar to the theoretical spectrum of CoO. Similarities are also observed between the spectra of $CZBrO_2$ and CZO_3 (after O_2 treatment) and the theoretical Co_2SiO_4. However, a simple qualitative comparison can be misleading since a peak in a Fourier transform spectrum can be due to different contributions which interfere with each other. Only a quantitative analysis will give an adequate description of the structure of the species inside the zeolite pores.

Figures 3−5 present the Fourier-transformed $\chi(k)\cdot k^3$ Co K-edge EXAFS functions of the three catalysts after O_2 and H_2 treatment together with the fitted curves. The low-frequency background and the high-frequency noise were reduced by

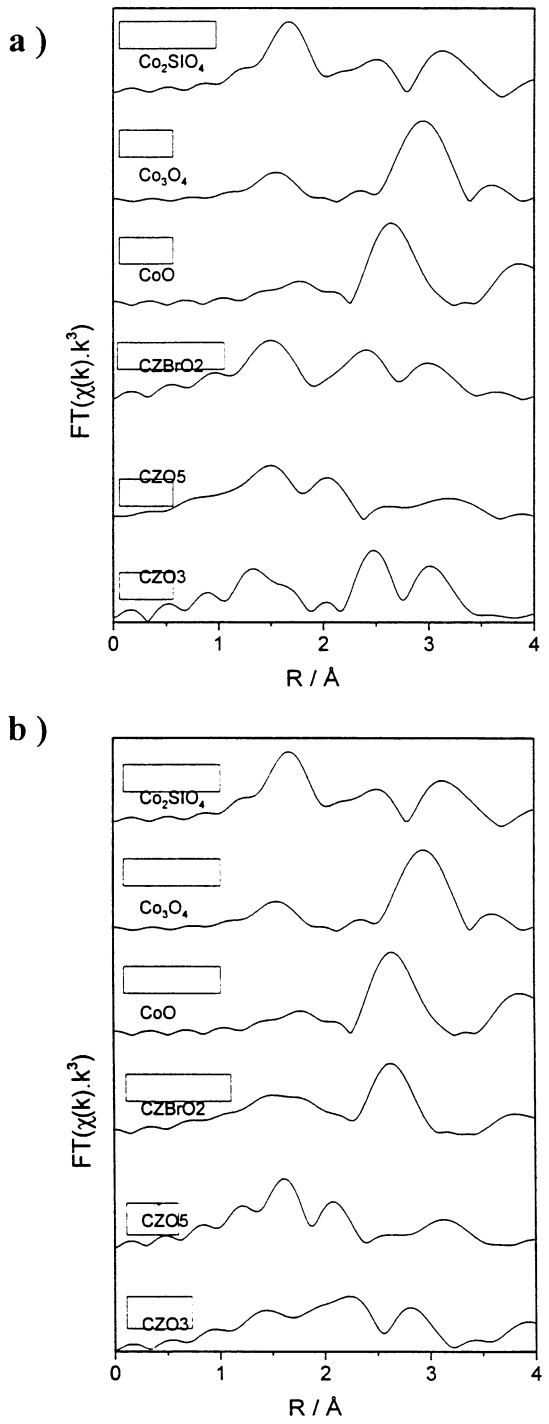

Figure 2. Co K-edge k^3-weighted Fourier transforms of the EXAFS functions of catalysts after treatment at 500 °C in O_2 (a) and H_2 (b). Simulated Co_2SiO_3, CoO, amd Co_3O_4 spectra are also presented for comparison.

applying Fourier filtering in the *R*-range interval between 0 and 4 Å using the inverse Fourier transformation. The solid lines represent the EXAFS data after filtering in the *R* range, whereas the dotted lines represent the results of the fit. The results of the quantitative analyses are given in Tables 1 and 2 with the real absorber−backscatterer distances since the distances observed in the Fourier-transformed spectra are always shorter than the real ones because of the phase shifts.

A detailed analysis of the fitting of each spectrum is presented in Figures 6−11. In these figures the contribution of each backscattering is separately presented on the overall spectrum.

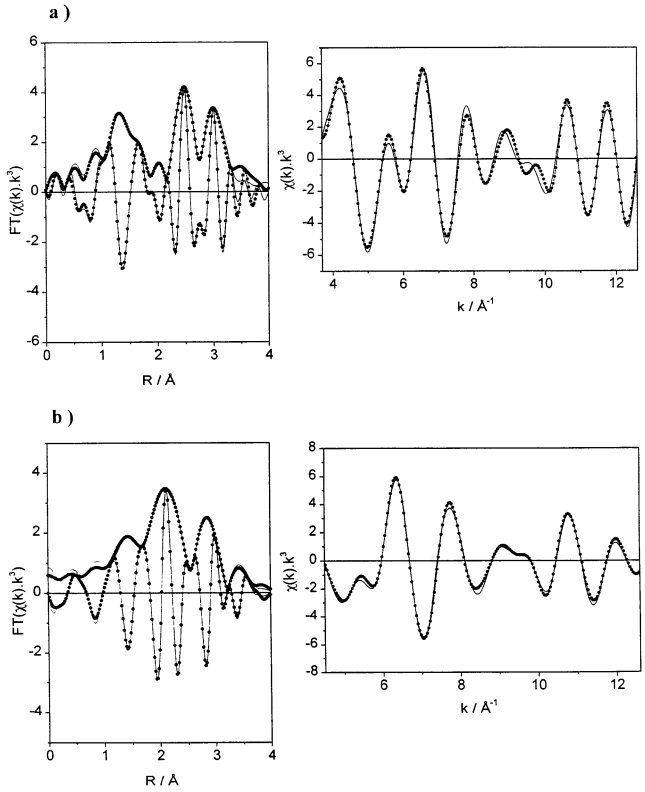

Figure 3. Fourier-transformed and k^3-weighted Co K-edge EXAFS function ($k^3 \cdot \chi(k)$) of the CZO3 catalyst after O_2 treatment (a) and after H_2 treatment (b): filtered measured data, light lines; curve-fitting results, dark lines.

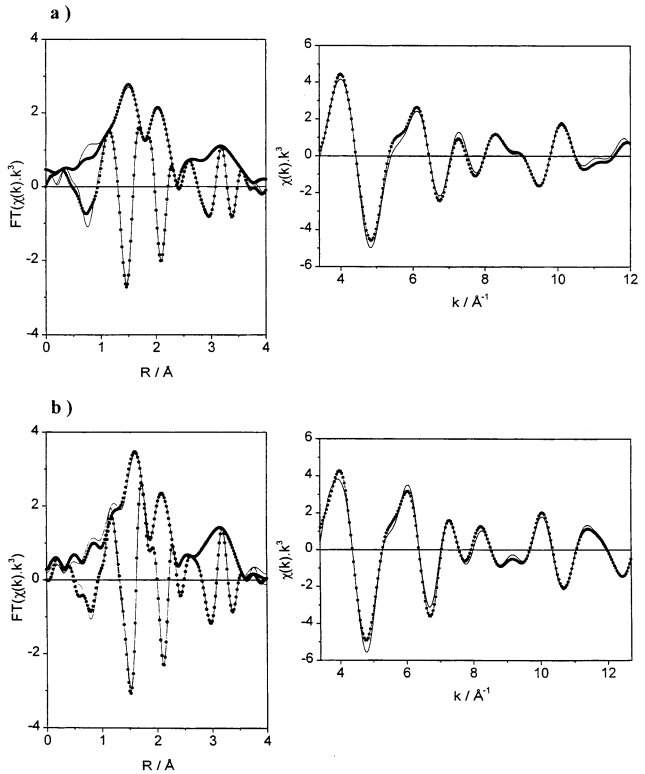

Figure 4. Fourier transformed and k^3-weighted Co K-edge EXAFS function ($k^3 \cdot \chi(k)$) of the CZO5 catalyst after O_2 treatment (a) and after H_2 treatment (b): filtered measured data, light lines; curve-fitting results, dark lines.

The first two bands in the FT of all catalysts were easily assigned to two Co−O shells (labeled Co−O(1) and Co−O(2)). The

TABLE 1: Results of the k^3-Weighted Curve Fittings of the Co K Edge of Co-MCI Catalysts after Treatment with O_2 (ΔR = 0−3.8 Å; Δk = 3.5−12.5 Å^{-1})

catalyst	shell	CN	R, Å	$\Delta\sigma^2$ 10^{-4} Å^2	$\Delta E°$, eV	ϵ_v^2	V_{IM}	V_{ABS}
CZO3	Co−O(1)	5.11	1.90	96	16	0.834	1.85	0.87
	Co−O(2)	0.26	2.20	−58	−16			
	Co−Co	4.98	2.95	27	−17			
	Co−Si/Al	2.78	3.19	−61	7.6			
CZO5	Co−O(1)	3.67	1.98	80	11	0.077	1.53	0.70
	Co−O(2)	1.53	2.32	11	−18			
	Co−Co(1)	0.82	2.94	80	9.7			
	Co−Co(2)	2.19	3.58	62	−6.9			
CZBrO2	Co−O(1)	3.22	1.96	28	2.7	0.191	2.11	1.35
	Co−O(2)	0.25	2.19	−90	−18			
	Co−Co	3.38	2.91	−2.7	−16			
	Co−Si/Al	5.71	3.15	−16	9.8			

TABLE 2: Results of the k^3-Weighted Curve Fittings of the Co K Edge of Co-MCI Catalysts after Treatment with H_2 (ΔR = 0−3.8 Å; Δk = 3.5−12.5 Å^{-1})

catalyst	shell	CN	R, Å	$\Delta\sigma^2$ 10^{-4} Å^2	$\Delta E°$, eV	ϵ_v^2	V_{IM}	V_{ABS}
CZO3	Co−O(1)	0.42	1.92	−58	−10	0.016	0.48	0.31
	Co−O(2)	6.30	2.12	80	−8.6			
	Co−Co	5.02	2.83	43	3.6			
	Co−Si/Al	4.83	3.10	−15	21			
CZO5	Co−O(1)	4.56	2.06	80	4.8	0.400	1.31	0.68
	Co−O(2)	0.56	2.37	−70	−21			
	Co−Co(1)	0.14	2.95	−38	14			
	Co−Co(2)	3.26	3.52	72	0.87			
CZBrO2	Co−O(1)	5.45	2.00	95	11	0.614	0.87	0.39
	Co−O(2)	0.53	2.20	−59	−21			
	Co−Co	4.90	3.00	45	−3.0			

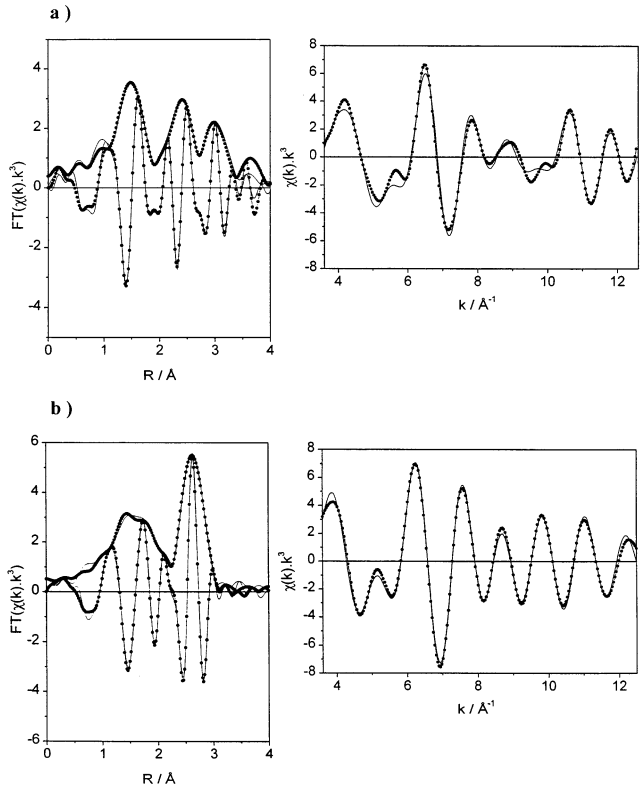

Figure 5. Fourier-transformed and k^3-weighted Co K-edge EXAFS function ($k^3 \cdot \chi(k)$) of the $CZBrO_2$ catalyst after O_2 treatment (a) and after H_2 treatment (b): filtered measured data, light lines; curve-fitting results, dark lines.

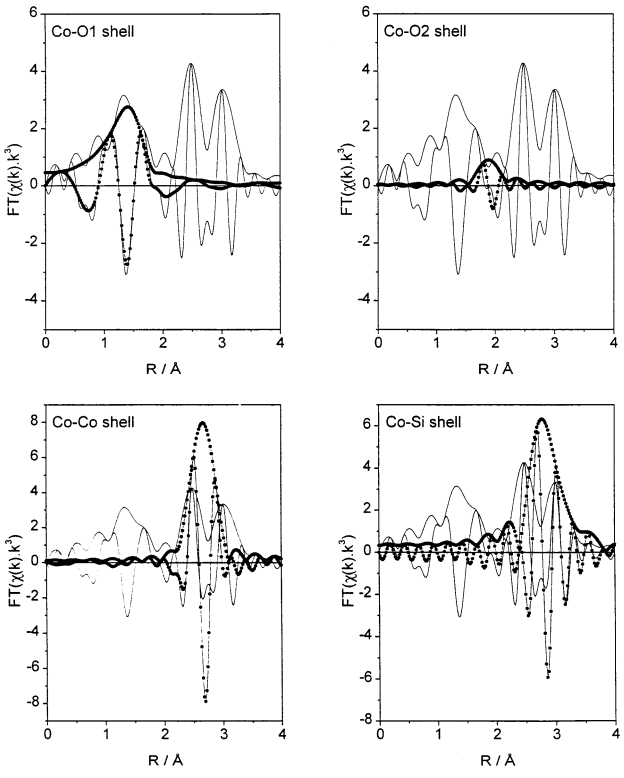

Figure 6. Detailed fitting analysis of the CZO3 catalyst after O_2 treatment: filtered measured data, dark lines; curve-fitting results of each shell, light lines.

(phase-corrected) Co−O distances vary between 1.9 and 2.2 Å, whereas larger bond distances (around 2.35 Å) were observed for the CZO5 catalyst. Additionally, the CZO5 catalyst displays a longer (phase-corrected) Co−Co distance near 3.5 Å, which is also found in the mixed octahedral/tetrahedral coordination in Co_3O_4. The smaller Co−Co bond distance found with CZBrO2, CZO3, and CZO5 is in the same range as the one obtained for CoO or Co_2SiO_4. Higher coordination numbers for the Co−Co contributions were consistently found when the

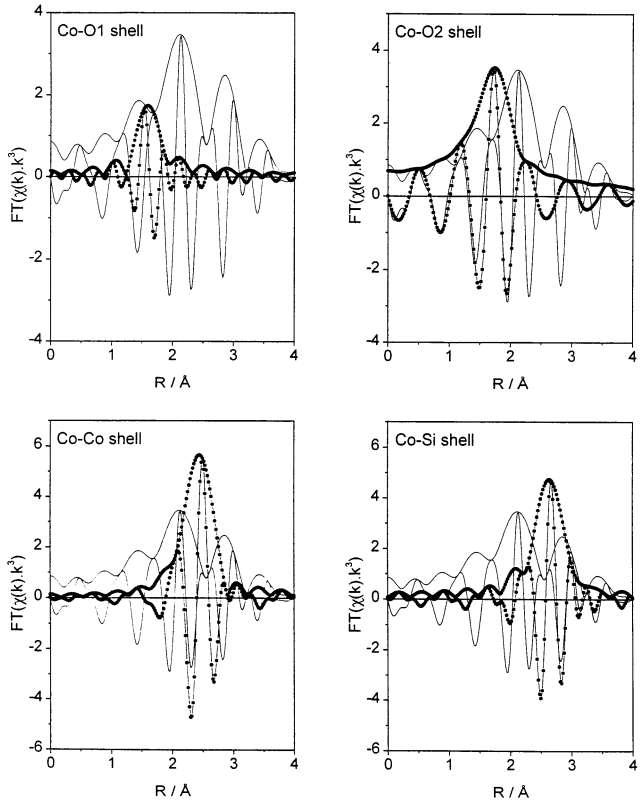

Figure 7. Detailed fitting analysis of the CZO3 catalyst after H_2 treatment: filtered measured data, light lines; curve-fitting results of each shell, dark lines.

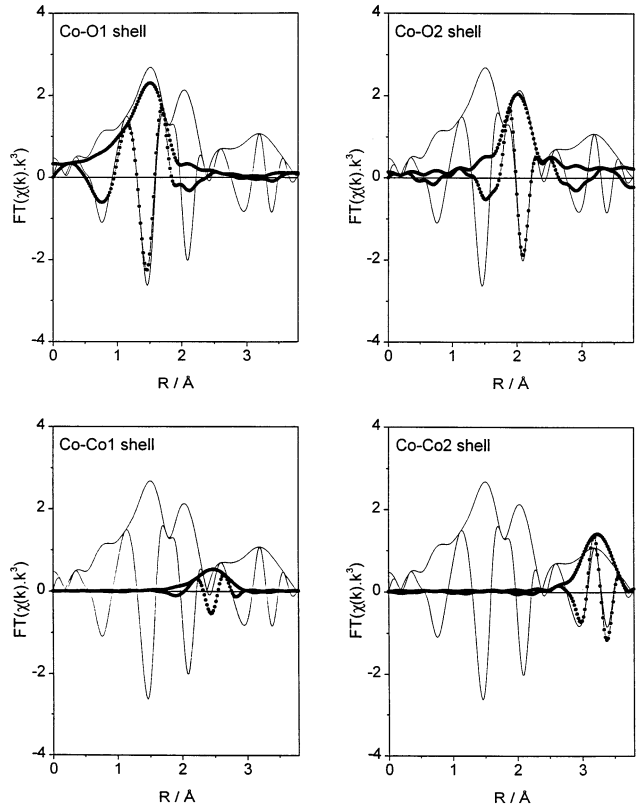

Figure 8. Detailed fitting analysis of the CZO5 catalyst after O_2 treatment: filtered measured data, light lines; curve-fitting results of each shell, dark lines.

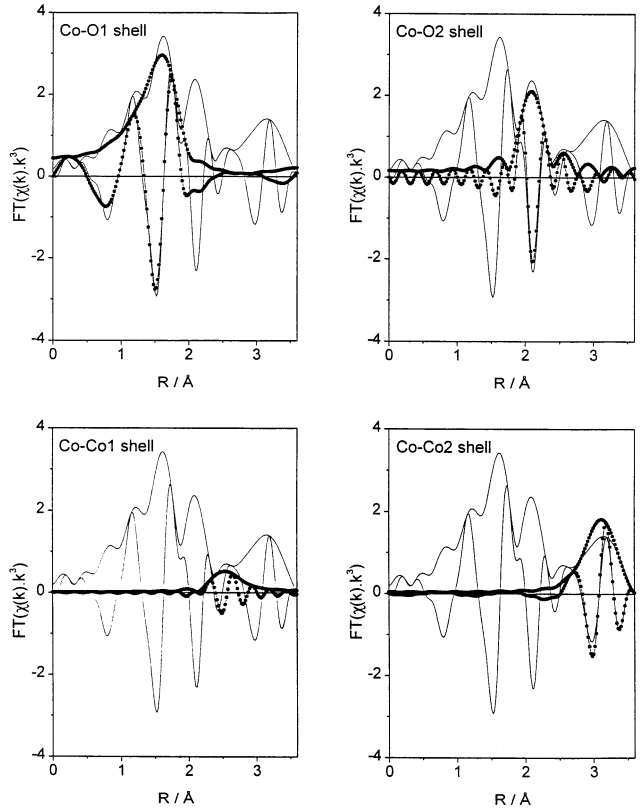

Figure 9. Detailed fitting analysis of the CZO5 catalyst after H_2 treatment: filtered measured data, light lines; curve-fitting results of each shell, dark lines.

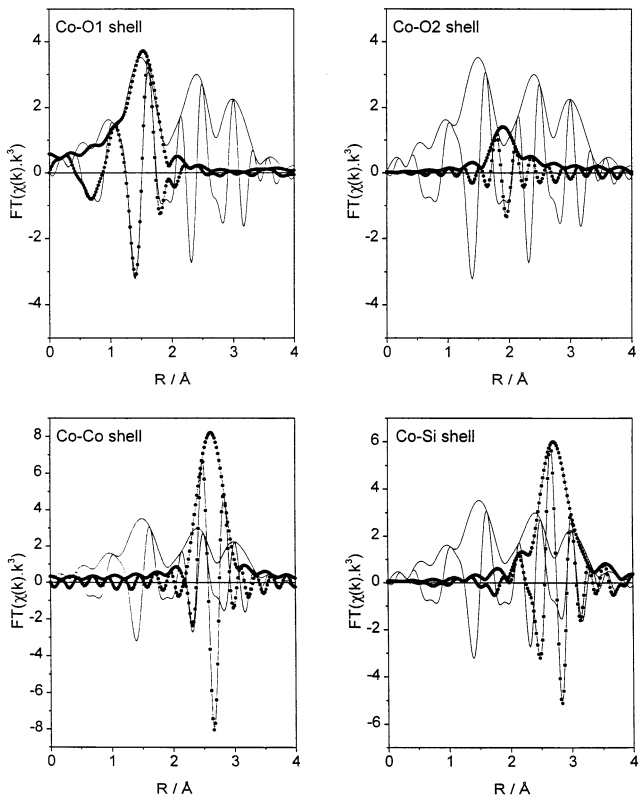

Figure 10. Detailed fitting analysis of the $CZBrO_2$ catalyst after O_2 treatment: filtered measured data, light lines; curve-fitting results of each shell, dark lines.

catalysts were treated with H_2, although they were still lower than the ones expected for a CoO crystal structure. Disorder and distortion effects can, however, cause an underestimation of the particle size.[9,10]

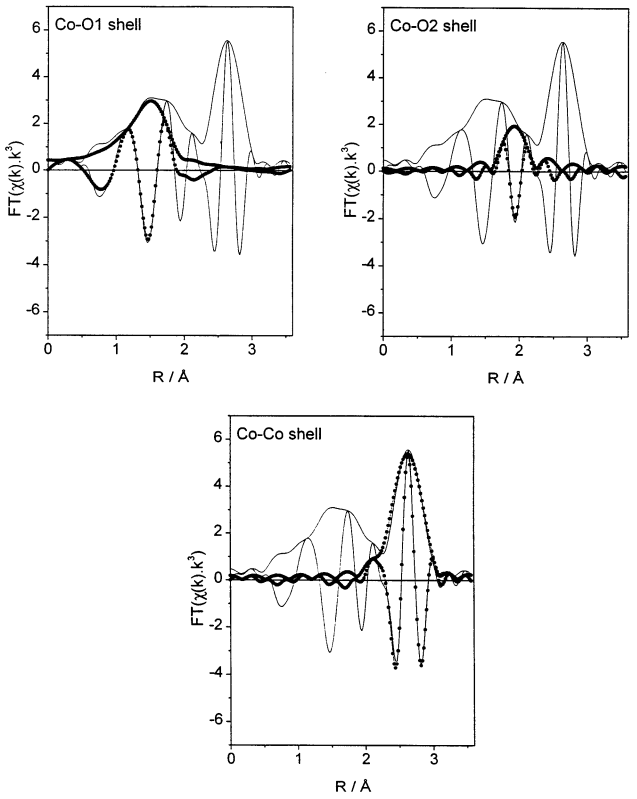

Figure 11. Detailed fitting analysis of the $CZBrO_2$ catalyst after H_2 treatment: filtered measured data, light lines; curve-fitting results of each shell, dark lines.

The assignment of the third and fourth shells was more difficult. A phase- and amplitude-corrected Fourier transform was applied to unambiguously distinguish the Co−Co distance from the Co−Si/Al contribution and to corroborate the given assignment. This method is based on the fact that a phase- and amplitude-corrected transform for a given absorber−backscatterrt pair must have a positive imaginary part peaking around the maximum of its magnitude.[11] Figures 12−14 show the phase- and amplitude-corrected Fourier transforms for three representative spectra. Figure 12 clearly shows that the third peak in the spectrum of $CZBrO_2$ after H_2 treatment corresponds to a Co−Co contribution rather than a Co−Si/Al contribution since the imaginary part peaks positive around the maximum for the Co−Co phase- and amplitude-corrected transform. The Co−Co phase- and amplitude-corrected transform (Figure 13a) and the Co−Si/Al phase- and amplitude-corrected transform (Figure 13b) of the third and fourth shells of the CZO3 catalysts treated with H_2 also corroborate the assignment of a Co−Co shell next to a Co−Si/Al shell. Figure 14 shows that both the third and fourth shells of the CZO5 catalyst are due to Co−Co contributions since again the imaginary part peaks positively for the Co−Co phase- and amplitude-corrected Fourier transform.

4. Discussion

Although the three catalyst samples of this study were prepared in a similar way by subliming a volatile cobalt halide onto the H form of the zeolite, their EXAFS characteristics reveal interesting differences which can by correlated with the catalytic performances and the responses to treatments in oxidizing or reducing atmospheres.

The largest Co−Co distance of 3.5 Å is found with the poorest catalyst after calcination. This distance is typical for

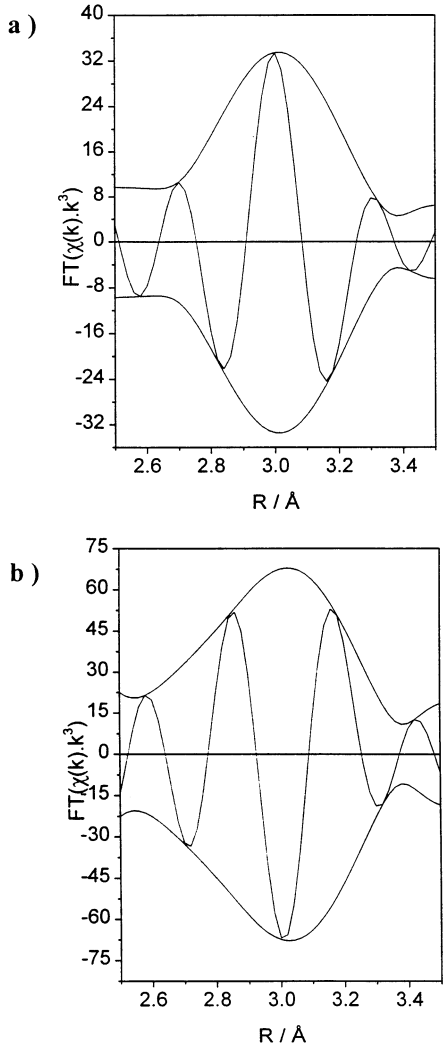

Figure 12. Co−Co (a) and Co−Si/Al (b) phase- and amplitude-corrected Co K-edge k^3-weighted Fourier transform of $CZBrO_2$ after H_2 treatment.

the Co_3O_4 crystal structure, where the distance between two Co^{2+} ions is known to be 3.5 Å. It has often been found that clusters of transition metals have a high catalytic activity for the (undesirable) combustion of hydrocarbons.[12] By consequence, such catalysts display a low selectivity for the (desired) interaction of the hydrocarbon with NO_x. Clearly, a catalyst with much Co in the form of Co_3O_4 clusters will show a low performance in NO_x reduction.

The TPR data in Figure 1 suggest that large Co_3O_4 particles are partially reduced at 400 °C. Indeed, the poor catalyst CZO5 is the only sample among those studied here which still displays a Co−Co distance of 3.5 Å. After treatment with H_2 at 300 °C a Co−Co distance of 3.0 Å or less is encountered in all samples subjected to H_2 treatment at 400 °C. This might indicate formation of Co^0 as found by Huffman et al.[13] and suggested by the TPR data, but this distance also exists in the material that was heated in O_2. A distance near 3 Å is compatible with formation of not only Co^0, but also CoO and dinuclear $[Co-O-Co]^{2+}$ ions. A value near 3 Å has been reported for the analogous dinuclear oxygen-bridged Fe complexes, in both Fe/MFI[11,14] and the MMO enzyme.[15] It is possible that reduction of Co_3O_4 clusters results in CoO as a primary product, which is then reduced further to Co^0. Remarkably, the coordination number for the Co−Co distance near 3 Å is near 5 for the

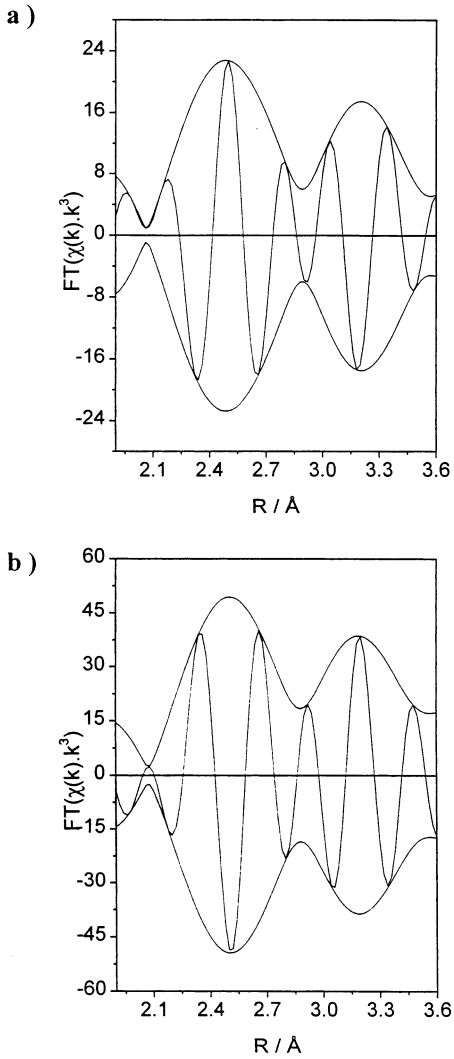

Figure 13. Co−Co (a) and Co−Si/Al (b) phase- and amplitude-corrected Co K-edge k^3-weighted Fourier transform of CZO3 after H_2 treatment.

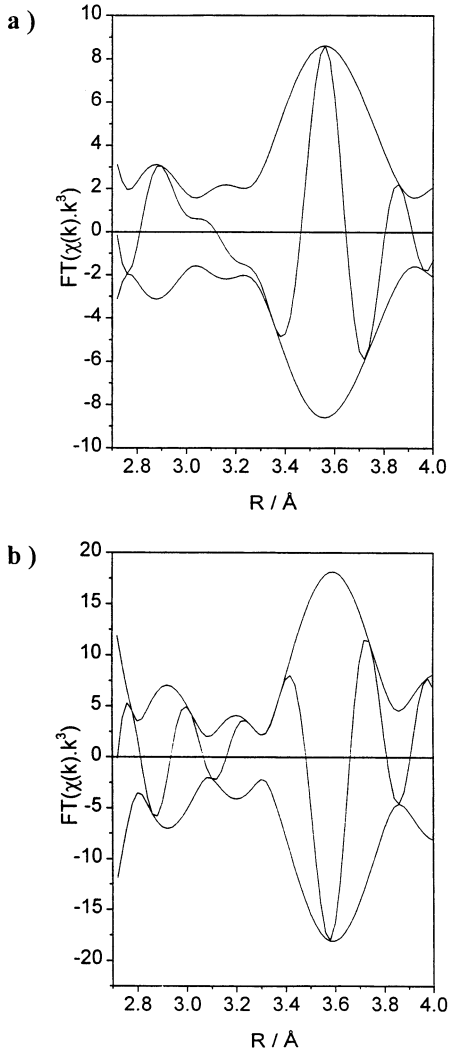

Figure 14. Co−Co (a) and Co−Si/Al (b) phase- and amplitude-corrected Co K-edge k^3-weighted Fourier transform of CZO5 after H_2 treatment.

partially reduced "good" catalysts CZO3 and $CZBrO_2$, but below 1 for the "poor" catalyst CZO5, which retains Co_3O_4 particles.

The interaction of Co with the T ions (T = Si or Al) in the zeolite framework is also of interest. It depends on the treatment and the nature of the Co species. With $CZBrO_2$ no interaction is apparent after H_2 reduction at 400 °C, but a high coordination number (∼6) of Co with T atoms is found after calcination in O_2. Reduction of part of the Co in this catalyst thus appears to result in less Co−T interaction. In contrast, with CZO3 the change of the Co−T coordination number caused by reduction is not accompanied by a significant change of the Co−Co coordination number.

As expected, both the calcined and the partially reduced samples contain a variety of Co species. Accordingly, two types of coordination of Co with oxygen appear necessary to obtain a satisfactory fit. If the Co^{2+} ions were only coordinated to oxygen of the zeolite framework, one might expect coordination numbers near 3 or 4. Higher CN values confirm the presence of oxo ions, oxide clusters, and Co−OH groups in the oxidized state. It is remarkable that the CN with nearest oxygen does not decrease upon reduction, though O atoms are undoubtedly removed during this treatment. To understand the high CN with oxygen of Co ions in the partially reduced CZO5 and $CZBrO_2$ catalysts, it should be mentioned that reduction at 400 °C is limited to oxo ions and some oxide clusters, while isolated Co^{2+} ions remain unreduced at this temperature. The water which is formed during reduction of the oxo species with hydrogen will thus react with the Co^{2+} ions, possibly hydrolyzing them, for instance

$$Co^{2+} + H_2O \rightleftarrows [Co{-}OH]^+ + H^+$$

as has often been observed for multivalent ions in zeolites. As a result the CN of these Co^{2+} ions with oxygen will increase, as observed for Co−O(1) in CZO5 and $CZBrO_2$ (see Tables 1 and 2).

The distribution of the oxygen atoms between the first and second shells, as well as the bond length, shows some variation depending on the pretreatment. These variations are probably due to the formation of very small or disordered Co species, since the deduced Co−O shells could only be fitted with very large Debye−Waller factors, which indicate a rather disordered system.

As mentioned above, the Co−Co distance of 3.5 Å in the poor catalyst CZO5 indicates the presence of fairly large Co_3O_4 particles. This is supported by the fact that this sample is unique by the absence of a Co−T coordination. In contrast, the Co−T coordination is high in $CZBrO_2$ and CZO3s with a Co−T distance of 3.15 Å in the calcined $CZBrO_2$(c) (Table 1). As these catalysts display Co−O bond distances between 1.9 and

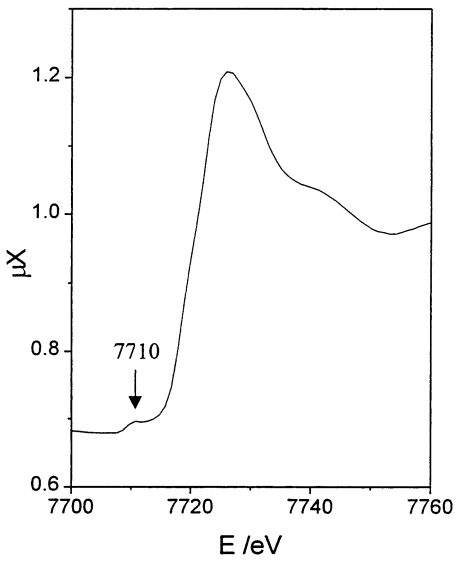

Figure 15. XANES region of CZO3 after H_2 treatment.

2.2 Å, as found in CoO and Co_2SiO_4, it appears that the Co ions occupy distinct positions with respect to the zeolite framework. The low Co−Co coordination number indicates small particles after reduction, though it is also possible that disorder or distortion effects are involved.

Information on the geometry of the Co particles being formed can be acquired from the near-edge region (XANES). A typical XANES spectrum is shown in Figure 15. A clear preedge peak appears at 7710 eV, which we ascribe, in agreement with the literature,[16] to an electric-dipole-forbidden, but quadrupole-allowed and vibronically allowed 1s → 3d electronic transition. Although a preedge feature is not expected for an octahedral environment, it could be due to a highly distorted octahedron.

5. Conclusions

The present data confirm that calcined Co/MFI samples prepared by sublimation are significantly affected by treatment in H_2 at 400 °C. This distinguishes such catalysts from others that are prepared by ion exchange from aqueous solution and are known to require much higher reduction temperatures. Treatment in oxygen at 400 °C of the present samples produces oxo species, in which the metal ions are coordinated both with framework and with extraframework oxygen. Accordingly, no data fit is possible by assuming only one set of Co−O distances. The data also indicate that rather large Co_3O_4 clusters were present in the poor catalyst CZO5. This is in line with the previous observations that transition-metal oxide particles possess high activity for the catalytic combustion of hydrocarbons, but a low selectivity for their interaction with NO_x.

Acknowledgment. This work was supported by the EMSI program of the National Science Foundation and the Department of Energy (Grant CHE-9810378) at the Northwestern University Institute for Environmental Catalysis. Financial aid from the Director of the Chemistry Division, Basic Energy Sciences, U.S. Department of Energy, Grant DE-FGO2-87ER13654, is gratefully acknowledged. We thank the staff of the SNBL at the ESFR for their technical support and kind help with the EXAFS measurements.

References and Notes

(1) Li, Y.; Armor, J. N. *Appl. Catal.* **1992**, *B1*, L31.
(2) Armor, J. N. *Catal. Today* **1995**, *26*, 147.
(3) Sobalík, Z.; Dedecek, J.; Ikonnikov, I.; Wichterlová, B. *Microporous Mesoporous Mater.* **1998**, 21.
(4) Dedecek, J.; Wichterlová, B. *J. Phys. Chem.* **1999**, *B103*, 1463.
(5) Wang, X.; Chen, H.-Y.; Sachtler, W. M. H. *Appl. Catal., B* **2000**, *26*, L227.
(6) Wang, X.; Chen, H. Y.; Sachtler, W. M. H. *J. Catal.* **2001**, *197*, 281−291.
(7) Vaarkamp, M.; Linders, J. C.; Koningsberger, D. C. *Physica B* **1995**, *209*, 159.
(8) Ankudinov, A. L.; Rehr, J. J. *Phys. Rev. B* **1997**, *56*, 1712.
(9) Shido, T.; Prins, R. *J. Phys. Chem. B* **1998**, *102*, 8426.
(10) Plazenet, G.; Cristol, S.; Paul, J. F.; Payen, E.; Lynch, J. *Phys. Chem. Chem. Phys.* **2001**, *3*, 246.
(11) Koningsberger, D. C.; Mojet, B. L.; van Dorssen, G. E.; Ramaker, D. E. *Top. Catal.* **2000**, *10*, 143.
(12) Chen, H.-Y.; Wang, X.; Sachtler, W. M. H. *Phys. Chem. Chem. Phys.* **2000**, *2*, 3083.
(13) Huffman, G. P.; Shah, N.; Zhao, J.; Huggins, F. E.; Hoost, T. E.; Halvorsen, S.; Goodwin, J. G., Jr. *J. Catal.* **1995**, *151*, 17.
(14) Marturano, P.; Drozdová, L.; Kogelbauer, A.; Prins, R. *J. Catal.* **2000**, *192*, 236.
(15) : Rosenzweig, A. C.; Nordlund, P.; Takahara, P. M.; Frederick, C. A.; Lippard, S. J. *Chem. Biol.* **1995**, *2*, 409.
(16) Shulman, R. G.; Yafet, Y.; Eisenberger, P.; Blumberg, W. E. *Proc. Natl. Acad. Sci. U.S.A.* **1976**, *73*, 1384.